JOINT INSTITUTE FOR NUCLEAR RESEARCH
Dzhelepov Laboratory of Nuclear Problems

FINAL REPORT ON THE INTEREST PROGRAMME

Radiation Protection and the Safety of Radiation Sources

Supervisor :	Dr. Said AbouElazm
Student :	Dhuha Ali
	El-Gammal, Egypt, Alexandria University.
Participation Period :	March 02 - April 19, Wave 14

Dubna, 2026

1 Abstract

Abstract—**Understanding of radiation measurements and protection methods involves the dealing with radiation detectors, which in fact need calibration to provide precise readings, and understanding the specification of energy resolution, which differ from one detector to another. Detectors as some kinds of scintillation detectors provides relatively poor resolution, detectors as semiconductors and pixels are advanced and more precise. Desired detectors were used in some applications for better understanding, including calculating of Alpha particle beam stopping range in air using pixel detector, and calculating of Gamma attenuation coefficient for copper and aluminum using BGO scintillation detector.**

Contents

1 Abstract **i**

2 Introduction **1**
2.1 Project Goals . . . 1
2.2 Background . . . 1

3 Scope of The Work and Methods **1**
3.1 Scope of the Work . . . 1
3.1.1 Radiation Sources . . . 1
3.1.2 Radiation Detectors . . . 1
3.1.3 Materials . . . 1
3.2 Methods . . . 1

4 Radiation Detection **2**
4.1 Scintillator Detectors . . . 2
4.1.1 BGO Detector . . . 2
4.1.2 NaI(Tl) Detector . . . 5
4.2 Semiconductor Detectors . . . 7
4.2.1 CdTe Detector . . . 7
4.3 Comparison between Scintillation Detector and Semiconductor Detector . . . 8
4.4 Pixel Detectors . . . 8
4.4.1 Determination of the Range of Alpha Particle in Air . . . 8

5 Determination of Gamma Ray Attenuation Coefficient Experimentally **9**

6 Conclusion **10**

A Acknowledgment **12**

B Gaussian Fit Spectra **12**

List of Figures

1 Schematic representation of the sequence of events [1, Fig.9-9] . . . 2
2 Co-60 spectrum Measured using BGO Detector . . . 3
3 Applied voltage vs. detector resolution for BGO . . . 3
4 spectra of Co-60 and Cs-137 . . . 4
5 The BGO Calibration Equation . . . 4
6 The spectrum of the Unknown Source 1 . . . 4
7 Co-60 spectrum using NaI(Tl) Detector . . . 5
8 Applied voltage vs. detector resolution for NaI(Tl) . . . 6
9 spectra of Co-60 and Cs-137 . . . 6
10 The NaI(Tl) Calibration Equation . . . 6
11 The spectrum of the Unknown Source 2 . . . 7
12 Spectrum recorded by CdTe Semiconductor Detector for Am-241 and Co-57 . . . 7
13 CdTe Detector Calibration Curve . . . 8
14 Alpha Beam Absorbed in Pixel Detector Simulation on SRIM-2013 . . . 8
15 Energy vs. Residual Range Relation from SRIM Simulation . . . 9
16 Cu : Relative Intensity Vs. Thickness . . . 10
17 Al : Relative Intensity Vs. Thickness . . . 10
B.1 Gaussian fits for BGO detector energy peaks at eight different applied voltages (from 1200V to 2000V). . . . 12
B.2 Gaussian fit to three well-known source peaks energies . . . 12
B.3 Gaussian fit to ^{60}Co photopeaks (1173 keV and 1332 keV) at five different applied voltages using NaI detector. . . . 13
B.4 Gaussian fit to three well-known source peaks energies measured using NaI(Tl) detector . . . 13
B.5 Identifying the peaks of unknown source 2 and making gaussian fit . . . 13

List of Tables

1 Scintillator Properties of Crystals 2
2 Statistical information and resolution for every applied voltage using BGO detector 3
3 Statistical information and resolution for every applied voltage using BGO detector 4
4 Calculating Peaks Energies Using Calibration Equation (3) 4
5 Comparing Peaks Energies of the Unknown Source to Eu-155 and Sm-153 Energies 5
6 The first peak Data: Statistical information and resolution for every applied voltage using NaI(Tl) detector 5
7 The second peak Data: Statistical information and resolution for every applied voltage using NaI(Tl) detector 5
8 Statistical information and resolution for every applied voltage using NaI(Tl) detector 6
9 Calculating Peaks Energies Using Calibration Equation (4) 7
10 Comparing Peaks Energies of the Unknown Source to Sb-125 Energies 7
11 Channels Information and Calculating Resolution for CdTe Detector 8
12 Recorded energies of Alpha particle at various distances from the absorber 8
13 Simulated Residual Range Values for Alpha Particles in Air 9
14 Cu Intensity-Thickness Data 10
15 Al Intensity-Thickness Data 10

2 Introduction

2.1 Project Goals

The goal of the project is to acquire basic practical skills for dealing with radiation safely, using radiation measurement tools, understanding how radiation detectors work and radiation interactions with matters. Acquiring basic knowledge about radiation protection and shielding, and dosimetry. Learning how to calculate the energy resolution and calibration of various detector types. Identifying unknown sources of radiation measured using the same detectors. Conducting experiments using advanced detectors to measure the distance covered by different radiation types and how to stop or reduce its catastrophic effects as a basic step in radiation shielding and protection.

2.2 Background

Radiation detection is based on the theory of interactions of radiation (Alpha particles and Gamma rays) with the materials of the detectors(scintillator crystals and absorbing materials). Gamma rays undergoes photoelectric effect and produces photoelectrons. Alpha particles lose their enegry continuously through coloumb interactions until all the particles are absorbed completely. The detectors measure the energy absorbed by their material and provide information in the form of analog signals to the energy possessed by the radiation. [1]

3 Scope of The Work and Methods

3.1 Scope of the Work

3.1.1 Radiation Sources

- Co-60
- Co-57
- Cs-137
- Am-241

3.1.2 Radiation Detectors

- BGO scintillation detector
- NaI(Tl) Scintillation detector
- CdTe semiconductor detector
- Pixel detector

3.1.3 Materials

- Air
- Copper
- Aluminum

3.2 Methods

- **Experimental Setups :** Radiation information is recorded as an analog signal by the detector, then is converted through an ADC device into digital signals, then the data is analyzed with a computer software and results are obtained.
- **Data Type Conversion Tools :** C++
- **Data Analysis Tools :** ROOT 5, Excel.
- **Data Analysis Methods :** Gaussian Fit Function, Statistical Information measurements and linking with physical meaning.
- **Simulation Tools :** SRIM-2013

4 Radiation Detection

4.1 Scintillator Detectors

Theory

Scintillator Detectors are energy transducers, converts the kinetic energy, represented in the motion of ionizing radiation particles, into flashes of light, going through a sequence of radiation interactions.

- **Interaction with the crystal** Gamma photons interact with the crystal through one of the three principal gamma interactions (photoelectric effect, compton scattering, or pair production).
- **Energy conversion** Fast electrons, then are produced as a result of these interactions. These electrons work on the excitation of the crystal atoms, the excited atoms emit photons in order to return back to the ground state.
- **Photomultiplier Tube (PMT)** The produced photons are incident on the cathode of the PMT and undergo photoelectric interaction to free up electrons. Then the electrons are accelerated and directed to collide with the Dynodes resulting in the free up of multiple electrons in a process of multiplication. All the electrons are then collected at the Anode of the PMT. The process of multiplication is repeated to obtain a strong pulse.

[2]

The scope of this study is to analyse, and compare between the two scintillator crystals of BGO and NaI(Tl).

Scintillator properties of crystals

Scintillator	Light output	Decay (ns)	Wavelength (nm) max	Density (g/cm2)	Hygroscopic
Na(Tl)	100	250	415	3.67	yes
CsI	5	16	315	4.51	slightly
BGO	20	300	480	7.13	no
BaF2(f/s)	3/16	0.7/630	220/310	4.88	slightly
CaF2	50	940	435	3.18	no
CdWO4	40	14000	475	7.9	no
LaBr3(Ce)	165	16	380	5.29	yes
LYSO	75	41	420	7.1	no
YAG(Ce)	15	70	550	4.57	no

FYS-KJM5920 - Nuclear Measurement Methods and Instrumentation 9

Table 1: Scintillator Properties of Crystals

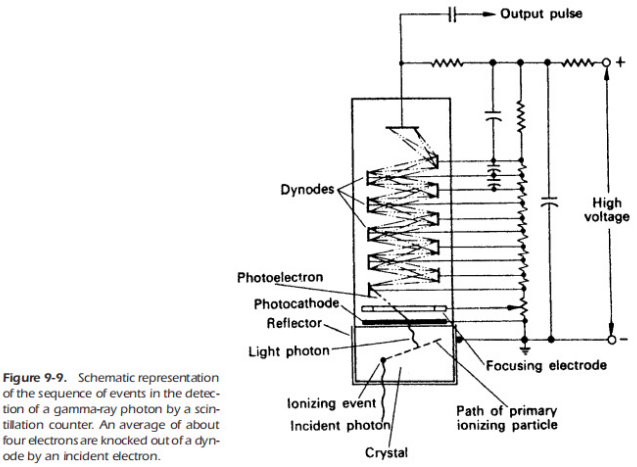

Figure 9-9. Schematic representation of the sequence of events in the detection of a gamma-ray photon by a scintillation counter. An average of about four electrons are knocked out of a dynode by an incident electron.

fig. 1: Schematic representation of the sequence of events [1, Fig.9-9]

DRS

An electronic chip which receives the micro-pulses from the anode and amplifies to ensure the peak voltage is within the range of the ADC. Its function is to convert the analog signals into digital in order to determine the maximum pulse height. Noise is filtered out through the discriminator, then the processed data,including pulse height and timestamp, are transmitted via USB/Ethernet interphase. Then the transmitted data is displayed using **ROOT 5** software. [3]

4.1.1 BGO Detector

Calculating Resolution

Co-60 was chosen as a radioactive source to conduct an experiment aiming to calculating the resolution of the BGO detector. It is well known that Co-60 spectrum has two distinctive peaks: one of energy $1173KeV$, the later is of $1332KeV$. [4]

1. **Data Analysis on ROOT 5:**

   In order to calculate the resolution, first a gaussian curve has to fit on the peaks appear in the spectrum to identify the required statistical information. To achieve that a **gaus** fit function is used on ROOT 5 Fit

panel. The fit information, including the mean and the sigma, is displayed on the fit canvas.

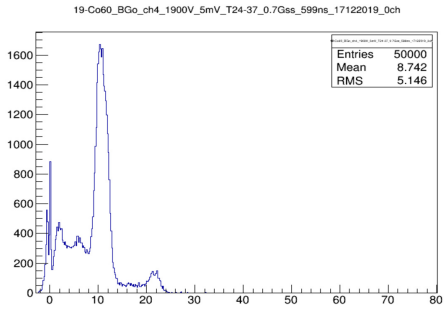

fig. 2: Co-60 spectrum Measured using BGO Detector

The **gaus** fit function is applied to all the peaks that appear in all the spectrums measured at different applied voltages (from $1200V$ to $2000V$). For more visualization of fits see fig.B.1 in the Appendix.

2. **Statistical Information and Calculating Resolution**
   - The **FWHM** of the peak is calculated through the equation :

$$\text{FWHM} = 2.355 \cdot \sigma \tag{1}$$

   - the resolution in percent is calculated through the equation :

$$\%R = \frac{FWMH}{mean} \times 100 \tag{2}$$

Voltage(V)	Mean	Sigma	Resolution(%)	FWHM
1200	1.609	0.458	66.99	1.078
1300	1.355	0.304	52.85	0.716
1400	1.924	0.295	36.11	0.695
1500	2.994	0.428	33.7	1.009
1600	4.401	0.633	33.88	1.491
1700	6.099	0.802	30.96	1.888
1900	10.66	1.237	27.33	2.913
2000	13.67	1.639	28.24	3.86

Table 2: Statistical information and resolution for every applied voltage using BGO detector

3. **Plots and Findings**

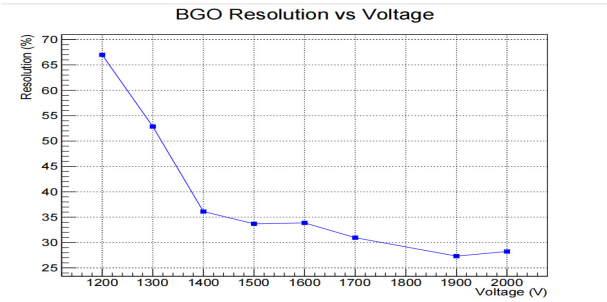

fig. 3: Applied voltage vs. detector resolution for BGO

The results are plotted as shown in fig.3. The best resolution is found to be 27.3% obtained when the applied voltage is $1900V$. As a consequence $1900V$ may be considered the optimum applied voltage to the BGO detector.

It is clear that this detector has poor resoultion, which also explaines why the spectrum of Co-60 appeared with only one peak although there have to be two peaks. The two peaks of the Co-60 are near to each other in energy, which might be overlapped if the radiation is measured using a poor resolution detector. [1]

Calibration

1. **Pulse Heights of Well-known standard Gamma Energies**

Energy calibration idea is based on the determination of the pulse height scale in terms of absolute gamma ray energies, through recording the pulse height spectrum of one or more standard gamma energies, and determining the position of the centers of peaks. Co-60 and Cs-137 are chosen as radioactive gamma emitters of standard known peaks energies [1]. For complete visualization of fits see fig. B.2 in the Appendix.

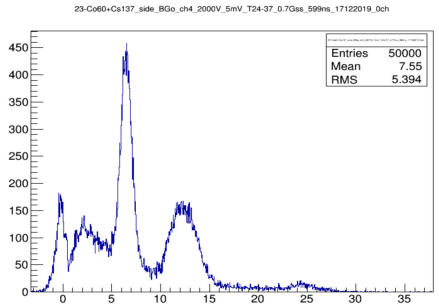

fig. 4: spectra of Co-60 and Cs-137

Energy (KeV)	(Channel)Mean	source
661.7	6.444	Cs137
1173.2	11.6	Co60
1332.5	13.32	Co60

Table 3: Statistical information and resolution for every applied voltage using BGO detector

2. The Calibration Equation

According to Knoll "The light output from a scintillator were perfectly proportional to energy deposited, then a calibration of pulse height (or centroid channel number in a multichannel analyzer) for the full-energy peak versus gamma-ray energy would be exactly linear." [1]

The calibration equation is expected to be a straight line equation for scintillation detectors. It can be extracted from the plot of **mean** against **Energy**, shown in fig. 5.

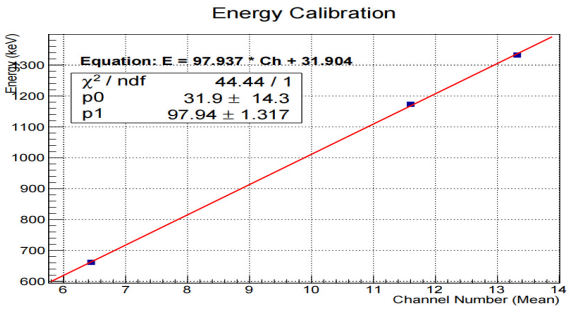

fig. 5: The BGO Calibration Equation

$$E = 97.937 \times \mathrm{Ch} + 31.904 \tag{3}$$

Determination of an Unknown Source 1

In order to identify the origin of an unknown source spectrum, The centers of the spectrum peaks are to be estimated using gaussian fit function on ROOT 5. The mean or the center of the peak represents the channel number, if it is substituted in the calibration equation of the detector by the mean of the unknown source, the energy of the peak radiation can be obtained.

1. **Statistical Information**

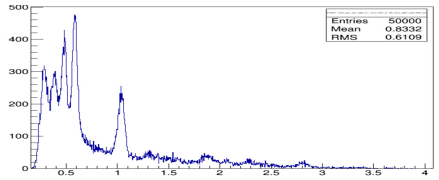

fig. 6: The spectrum of the Unknown Source 1

peak no.	Mean(Ch)	Error(Ch)	Error in energy(KeV)	Energy(KeV)
1	0.254	0.001	0.108	56.780
2	0.3815	0.001	0.137	69.267
3	0.4774	0.001	0.069	78.659
4	0.5825	0.001	0.049	88.952
5	1.032	0.001	0.098	132.975

Table 4: Calculating Peaks Energies Using Calibration Equation (3)

2. **Findings 1**

The spectrum obtained by BGO detector to the unknown source has five energy peaks. Their energies are calculated from the calibration equation (3), and then are compared to Eu-155 and Sm-155, Eu-155 has five close energies to the original source's with difference of few KeV, in which two of them may appear overlapping in the spectrum of BGO, this will be explained by the poor resolution. However, the source is more likely to be Sm-153 than Eu-155, the difference in energies is less, and it can be noted that it has a mostly identical energy to the unknown source $69KeV$. [4]

Energy(KeV)	Eu155	Difference	Sm153	Difference
56.780	45.299	11.372998		
69.267	60.0086	9.1212537	69.67301	0.5431563
78.659			83.36716	4.6394803
88.952	86.0591, 86.5479	2.355434	89.48593	0.484659
132.975	105.3083	27.568747	103.18007	29.696977

Table 5: Comparing Peaks Energies of the Unknown Source to Eu-155 and Sm-153 Energies

4.1.2 NaI(Tl) Detector

Calculating Resolution

1. **Data Analysis on ROOT 5:**

The same procedures which have been followed on calculating BGO resolution are repeated for the NaI(Tl) detector, including gaussian fit and the extraction of the statistical information. This time two peaks are seen clearly in the spectrum, the gaussian fit is done for both. See fig.B.3 for visualizing fit details.

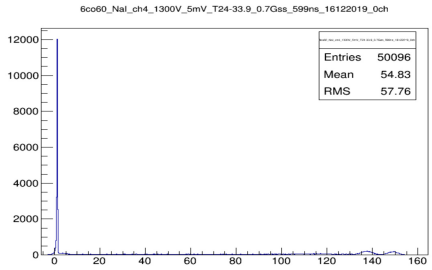

fig. 7: Co-60 spectrum using NaI(Tl) Detector

2. **Statistical Information and Calculating Resolution**

The FWHM and the resolution in percentage are calculated for each peak for the five different applied voltages. Through equations (1) and (2).

Applied Voltage (V)	Mean	Sigma	FWHM	Resolution(%)
900	23.67	0.6368	1.4869	6.28
1000	40.64	0.9908	2.3135	5.69
1100	65.77	1.532	3.5772	5.44
1200	98.64	2.19	5.1137	5.18
1300	137.4	2.639	6.1621	4.48

Table 6: The first peak Data: Statistical information and resolution for every applied voltage using NaI(Tl) detector

Applied Voltage (V)	Mean	Sigma	FWHM	Resolution(%)
900	26.57	0.6234	1.4681	5.53
1000	45.46	0.9995	2.3538	5.18
1100	73.26	1.541	3.6291	4.95
1200	108.5	1.937	4.5616	4.20
1300	148.8	2.471	5.8192	3.91

Table 7: The second peak Data: Statistical information and resolution for every applied voltage using NaI(Tl) detector

3. **Plots and Findings**

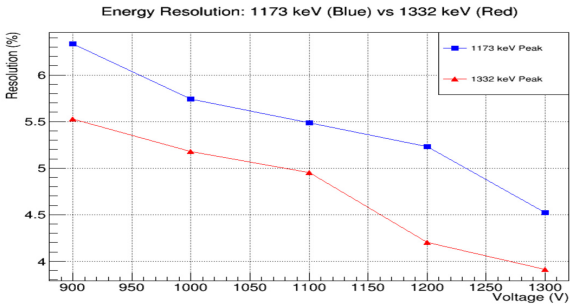

fig. 8: Applied voltage vs. detector resolution for NaI(Tl)

When plotting the applied voltage against the calculated resolution, the best resolution is found to be 3.9%. NaI(Tl) is considered to have a good resolution. A NaI(Tl) detector provided a better energy resolution than a BGO detector.

Calibration

1. **Pulse Heights of Well-known standard Gamma Energies**

Co-60 and Cs-137 are chosen for calibration. The gaussian curve is fitted on the peaks to determine the position of their pulse amplitude as explained before.

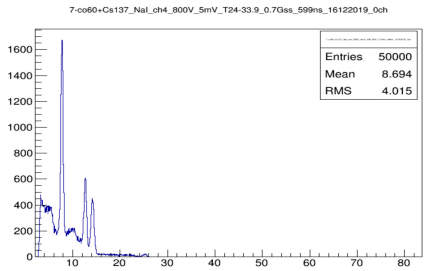

fig. 9: spectra of Co-60 and Cs-137

Energy(KeV)	Mean(Channel)	source
661.7	7.693	Cs137
1173.2	12.62	Co60
1332.5	14.13	Co60

Table 8: Statistical information and resolution for every applied voltage using NaI(Tl) detector

2. **The Calibration Equation**

The calibration equation is expected to be a straight line equation for scintillation detectors. It can be extracted from the plot of **mean** against **Energy**, shown in fig. 9.

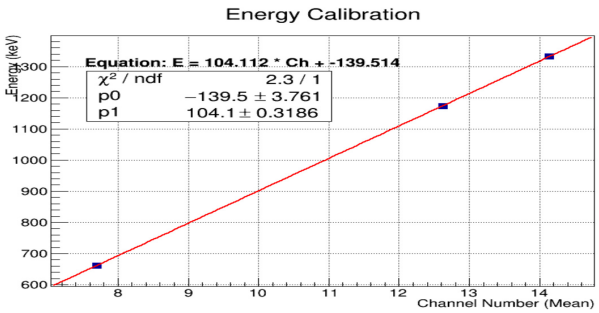

fig. 10: The NaI(Tl) Calibration Equation

$$E = 104.112 \times \text{Ch} - 139.514 \tag{4}$$

Determination of an Unknown Source 2

1. **Statistical Information**

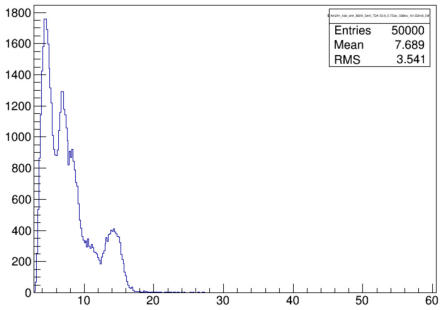

fig. 11: The spectrum of the Unknown Source 2

peak no.	Mean(Ch)	Error(Ch)	Error in energy(KeV)	Energy(KeV)
1	4.699	0.008	0.833	349.6519±0.8328
2	6.899	0.025	2.603	578.6719±2.6025
3	7.785	0.095	9.890	670.9045±9.8895

Table 9: Calculating Peaks Energies Using Calibration Equation (4)

2. **Findings 2**

The peak energies which are calculated from the calibration equation (4), listed in Table 7, are compared to Sb-125's [4]. One peak energy of $670.9KeV$ is mostly identical to Sb-125's $671.4KeV$. Two other peaks are likely close with energy difference of $19KeV$ and $30KeV$. The unknown source 2 is likely to be Sb-125.

Energy(KeV)	Sb125	Difference
349.6519±0.8328	380.452	29.967
578.6719±2.6025	600.597	19.323
670.9045±9.8895	671.4	0.495

Table 10: Comparing Peaks Energies of the Unknown Source to Sb-125 Energies

4.2 Semiconductor Detectors

Where the only way to reduce the statistical limit of energy resolution is to increase the number of information carriers, semiconductor detectors are characterized by producing a great number of information carriers per pulse compared to other detectors.They can provide the best energy resolution among the other types. They provide more advantages as compact size and fast timing characteristics. From examples of widely used semiconductor detectors are silicon and germanium detector. The scope of this study concentrates on another kind of semiconductor detectors which is CdTe. [1]

4.2.1 CdTe Detector

The used model of CdTe detector in conducting this experiments is X-123CdTe, as mentioned before about the semiconductor detector, it is characterized by the relatively compact size of $(7 \times 10 \times 2.5cm^3)$. The single interaction with X-ray or gamma ray produces one electron/hole pair for every $4.3eV$ energy lost in CdTe, compared to the scintillator detectors which produce one photoelectron for every $100eV$ energy lost, which results in characterizing by a better energy resolution [5].

Calculating Resolution and Plotting Calibration Curve

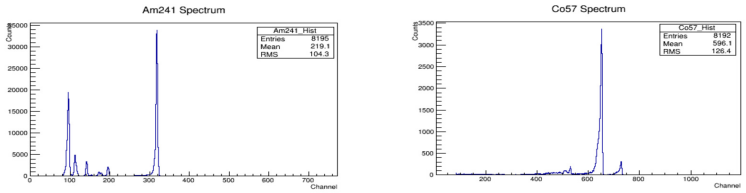

fig. 12: Spectrum recorded by CdTe Semiconductor Detector for Am-241 and Co-57

CdTE detector was used to record Two of the standard gamma sources radiations, Co-57 and Am-241. It is noticed clearly that peaks widths are narrower than that were recorded by the scintillator detectors, a better energy resolution is expected.

Am-241				
Peak Standard Energy(KeV)	sigma	Mean(Ch)	FWHM	%R
26.345	2.775	94.65	6.535125	6.90
33.196	2.854	113	6.72117	5.95
59.541	2.194	317.7	5.16687	1.63
Co-57				
Peak Standard Energy(KeV)	sigma	Mean(Ch)	FWHM	%R
14.413	4.79	528.7	11.28045	2.13
122.061	3.706	649.6	8.72763	1.34
136.474	4.156	725.5	9.78738	1.35

Table 11: Channels Information and Calculating Resolution for CdTe Detector

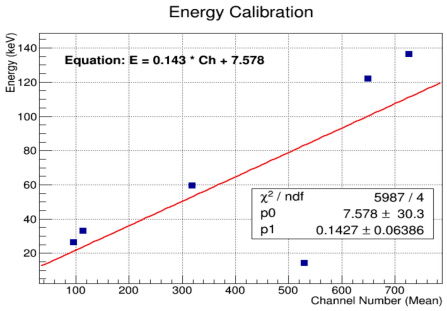

fig. 13: CdTe Detector Calibration Curve

FWHM and %R are calculated from (1) and (2). The calibration curve is drawn based on the standard energies of Am-241 and Co-57 to find the calibration equation to be:

$$E = 0.143Ch + 7.578 \tag{5}$$

4.3 Comparison between Scintillation Detector and Semiconductor Detector

As The experimental results showed in the previous sections of this report, the main point of comparison is about the energy resolution. Scintillator detectors, like NaI(Tl) and BGO were found to provide a relatively poor energy resolution spectrum. The best energy resolution achieved was 3.9% for NaI(Tl)7, while BGO resolution calculations were much worse2. The CdTe detector provided better energy resolution values, with a best energy resolution achieved of 1.34%. 11

4.4 Pixel Detectors

4.4.1 Determination of the Range of Alpha Particle in Air

The experiment using pixel detector is based on the theory of the specific Alpha particle range in matter. Alpha particle have energy loss characteristics, the range of the Alpha particle in an absorbing material depends on the number of interactions it undergoes through the absorber path, Alpha particle will have a definite distance that can travel before its kinetic energy drops to zero and it stops completely. [1]

The aim of the study is to conduct this experiment using pixel detector in lab and comparing the results to the simulation on **SRIM-2013** software. The absorbing medium is air and the Alpha is of energy $4MeV$, the available Alpha source to be used is Am-241.

Using Pixel Detector

Range (mm)	0	2	4	6	8	10	12	14	16
Energy(KeV)	3694	3432	3204	2897	2835	2340	2281	1962	1587

Table 12: Recorded energies of Alpha particle at various distances from the absorber

The Alpha source is placed at a distance away from the detector and the energy absorbed by the pixel detector is recorded, representing the residual energy after some of its energy is absorbed by air. The residual energy of Alpha particle beam is recorded at various distances from the detector, which mean that $3694KeV$ at zero distance from the detector represents the energy absorbed by the detector from the $4MeV$ Alpha beam.

Monte Carlo Simulation

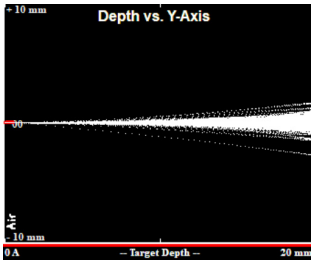

fig. 14: Alpha Beam Absorbed in Pixel Detector Simulation on SRIM-2013

The procedures are reversed in the simulation on SRIM-2013. An absorber width is assumed, must exceed the expected range corresponding to every energy obtained from the practical results, then the actual residual range of Alpha beam is measured.

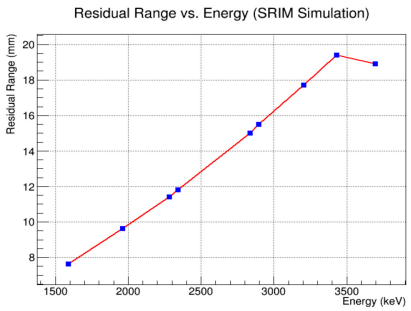

fig. 15: Energy vs. Residual Range Relation from SRIM Simulation

Energy(KeV)	3694	3432	3204	2897	2835	2340	2281	1962	1587
Residual Range (mm)	18.9	19.4	17.7	15.5	15.0	11.8	11.4	9.62	7.64

Table 13: Simulated Residual Range Values for Alpha Particles in Air

Findings

The results shows that there is a direct relation between the residual energy in pixel detector and the residual expected range of Alpha to stop in air. When the source was away from the detector by $10mm$ the residual energy in the detector was $2340KeV$, when adding this value to the residual range expected by the simulation the range is found to be $21.8mm$, the Alpha beam which possesses that amount of energy has to cut a distance of $11.8mm$ to stop completely in air.

5 Determination of Gamma Ray Attenuation Coefficient Experimentally

Introduction

Gamma rays are more likely to have a single interaction, they are either fully absorbed in the absorber or are scattered by large angles. The number of gamma photons which manage to transmit through the absorber are given in terms of number of incident photons I_o, are calculated through this equation [1]:

$$I = I_o e^{-\mu t} \tag{6}$$

In terms of radiation shielding, the most common way is to surround the source with a thick layer of a shielding material to reduce the effect of the radiating material as much as possible. In this experiment, Al and Cu are been used as a absorber while varying the thickness and recording the radiation spectrum using BGO scintillator detector. [1]

According to Knoll "The total area under the peak, above any background, is the most common measure of the intensity of the corresponding gamma ray." [1] For Every recorded spectrum signal, a gaussian curve is fitted and the area under the curve is extracted (using ROOT 5 software). Then the intensity is calculated through the equation:

$$I = constant \times sigma \times \sqrt{2\pi} \tag{7}$$

Relative Intensity-Thickness Data and Plots

The calculated intensities from (7) are substituting in (6), then the relation between the relative intensity and the absorber thickness is represented in the plot, in order to calculate the attenuation coefficient μ.

Copper Shield

Thickness x (cm)	constant	sigma	intensity I	ln(Io/I)
0	1255	1.494	4699.853	0
0.095	1476	1.201	4443.44	0.0561
0.15	1511	1.175	4450.331	0.0546
0.18	1472	1.203	4438.777	0.0572
0.3	1437	1.225	4412.48	0.0631
0.45	1453	1.213	4417.905	0.0619
0.6	1395	1.267	4430.378	0.059
0.75	1349	1.294	4375.585	0.0715
0.9	1352	1.278	4331.093	0.0817
1.08	1332	1.295	4323.783	0.0834
1.26	1310	1.301	4272.072	0.0954

Table 14: Cu Intensity-Thickness Data

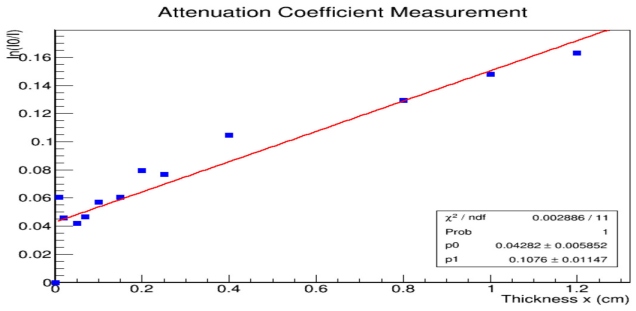

fig. 16: Cu : Relative Intensity Vs. Thickness

Attenuation coefficient of Cu =The slope of the straight line=0.1076

Aluminum Shield

Thickness x (cm)	constant	sigma	intensity I	ln(Io/I)
0	1255	1.494	4699.853	0
0.095	1476	1.201	4443.44	0.0561
0.15	1511	1.175	4450.331	0.0546
0.18	1472	1.203	4438.777	0.0572
0.3	1437	1.225	4412.48	0.0631
0.45	1453	1.213	4417.905	0.0619
0.6	1395	1.267	4430.378	0.059
0.75	1349	1.294	4375.585	0.0715
0.9	1352	1.278	4331.093	0.0817
1.08	1332	1.295	4323.783	0.0834
1.26	1310	1.301	4272.072	0.0954

Table 15: Al Intensity-Thickness Data

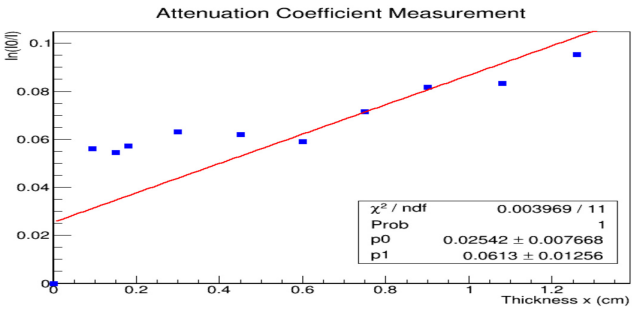

fig. 17: Al : Relative Intensity Vs. Thickness

Attenuation coefficient of Al =The slope of the straight line=0.0613

Comparing Between Copper and Aluminum in Shielding

The results show that copper has an attenuation coefficient greater than that of Aluminum, which supports the fact that high-Z materials are much more effective in shielding of gamma rays than low-Z materials. [1]

6 Conclusion

The practical results successfully showed a verification to the theoretical expectations. When studying the desired detectors, semiconductor detectors showed a relatively better energy resolution compared scintillation detectors. Pixel detectors are more advanced and showed a greater ability to record more information within an event.

In terms of shielding and protection from radiation, the materials of more charge dense showed a greater ability to attenuate the gamma radiation. And for Alpha beam, air successfully managed to stop it at a relatively short distance.

References

[1] G. F. Knoll, *Radiation Detection and Measurement*, 4th ed. Hoboken, NJ: John Wiley & Sons, 2010.

[2] H. Cember and T. E. Johnson, *Introduction to Health Physics*, 4th ed. New York: McGraw-Hill Medical, 2009.

[3] Laboratory Equipment Division, *Digital Readout System (DRS) User Manual/Technical Guide*, Nuclear Physics Laboratory, 2026, accessed via provided laboratory documentation.

[4] International Atomic Energy Agency, "Update of x ray and gamma ray decay data standards for detector calibration and other applications," https://nds.iaea.org/xgamma_standards/genergies1.htm, 2007, accessed: 2026-04-21.

[5] Amptek Inc., *X-123CdTe: Complete X-Ray and Gamma-Ray Spectrometer*, Amptek Inc. - Ametek Materials Analysis Division, 14 DeAngelo Drive, Bedford, MA 01730-2204 U.S.A., 2026, technical Specifications and Interface Software Description. [Online]. Available: http://www.amptek.com

A Acknowledgment

I would like to express my deepest gratitude to my supervisor **Dr.Said AbouElazm** for his academic support, and for providing the necessary insights to conduct these experiments successfully.
I am also grateful to the JINR University Centre staff for giving me the opportunity to participate in this project, which has significantly enhanced my practical skills and understanding of radiation detection and measurement. This work would not have been possible without the excellent resources and the supportive environment provided by the center.

B Gaussian Fit Spectra

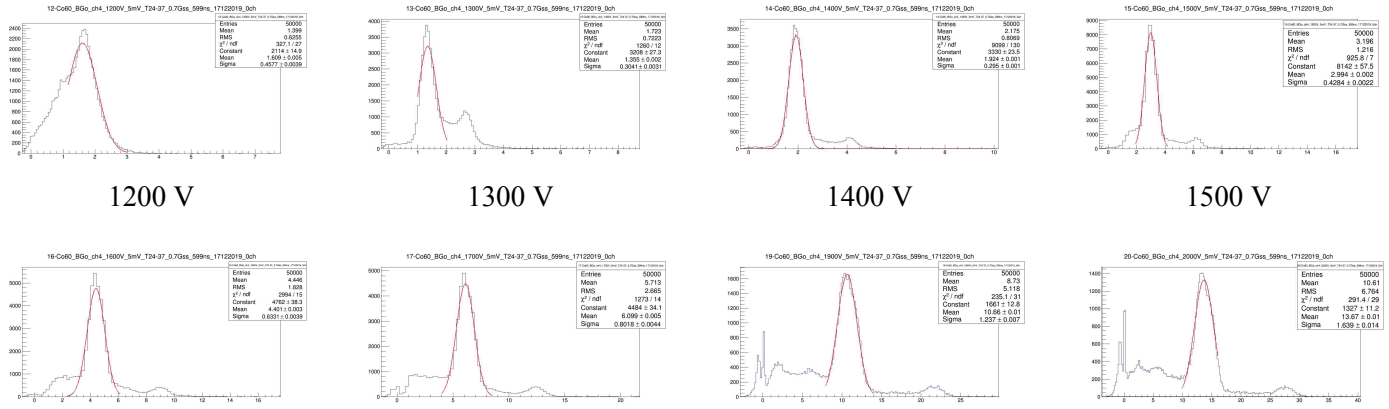

1200 V 1300 V 1400 V 1500 V

1600 V 1700 V 1900 V 2000 V

fig. B.1: Gaussian fits for BGO detector energy peaks at eight different applied voltages (from 1200V to 2000V).

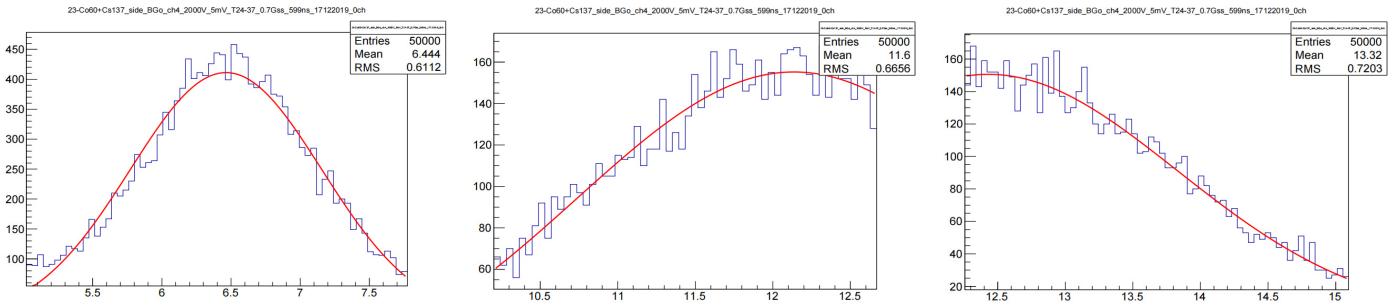

Cs-137 $662KeV$ Co-60 $1173KeV$ Co-60 $1332KeV$

fig. B.2: Gaussian fit to three well-known source peaks energies

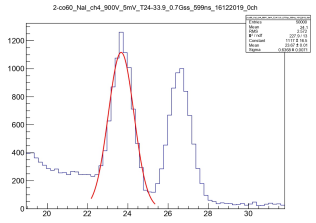

First peak, 900V

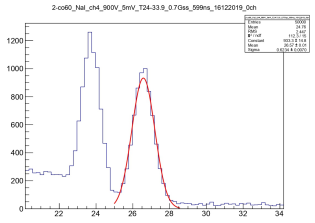

Second peak, 900V

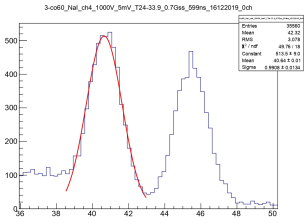

First peak, 1000V

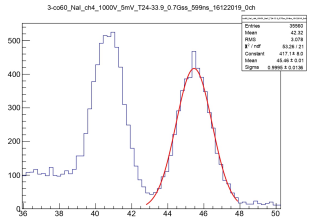

Second peak, 1000V

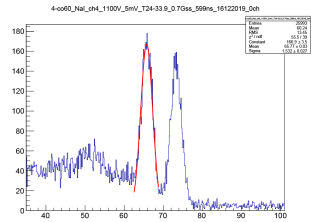

First peak, 1100V

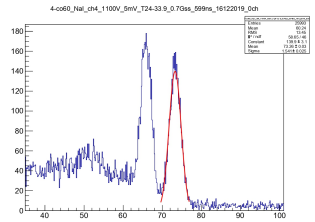

Second peak, 1100V

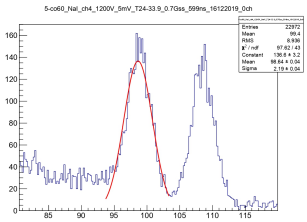

First peak, 1200V

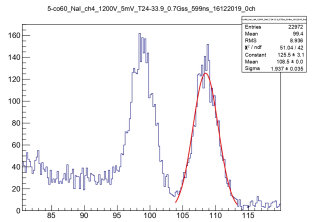

Second peak, 1200V

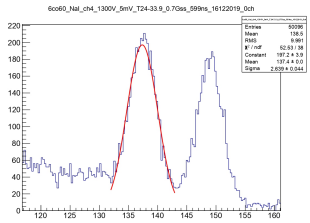

First peak, 1300V

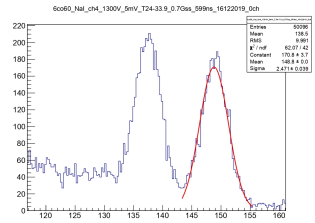

Second peak, 1300V

fig. B.3: Gaussian fit to ^{60}Co photopeaks (1173 keV and 1332 keV) at five different applied voltages using NaI detector.

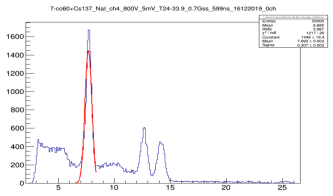

Cs-137 $662KeV$

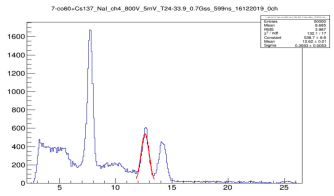

Co-60 $1173KeV$

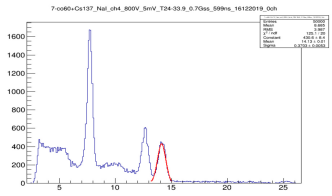

Co-60 $1332KeV$

fig. B.4: Gaussian fit to three well-known source peaks energies measured using NaI(Tl) detector

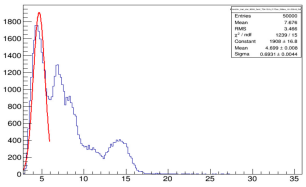

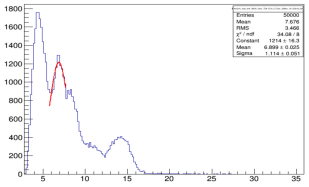

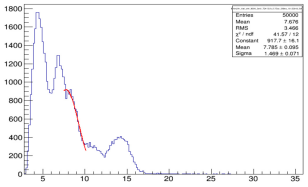

fig. B.5: Identifying the peaks of unknown source 2 and making gaussian fit